Cellular and Molecular Biology
E-ISSN : 1165-158X / P-ISSN : 0145-5680
www.cellmolbiol.org

Investigating STEAP2 as a potential therapeutic target for the treatment of aggressive prostate cancer.

Leia A. Jones[1], Gillian E Conway[1], Aimy Nguyen-Chi[1], Stephanie Burnell[1,2], Gareth J. Jenkins[1], R. Steven Conlan[1], Shareen H. Doak[1,*]

[1] Institute of Life Science, Swansea University Medical School, Faculty of Medicine, Health and Life Sciences, Singleton Park, Swansea, SA2 8PP, Wales, UK

[2] Cardiff Institute of Infection & Immunity, Cardiff University, Cardiff, CF10 3AT, Wales, UK

ARTICLE INFO

Original paper

Article history:
Received: February 18, 2023
Accepted: April 20, 2023
Published: April 30, 2023

Keywords:

Prostate cancer, STEAP2, biomarker, CRISPR/Cas9, antibody, proliferation, metastasis, invasion

ABSTRACT

The expression of six transmembrane epithelial antigen of the prostate (STEAP2) is increased in prostate cancer when compared to normal tissue, suggesting a role for STEAP2 in disease progression. This study aimed to determine whether targeting STEAP2 with an anti-STEAP2 polyclonal antibody (pAb) or CRISPR/Cas9 knockout influenced aggressive prostate cancer traits. Gene expression analysis of the *STEAP* gene family was performed in a panel of prostate cancer cell lines; C4-2B, DU145, LNCaP and PC3. The highest increases in *STEAP2* gene expression were observed in C4-2B and LNCaP cells ($p<0.001$ and $p<0.0001$ respectively) when compared to normal prostate epithelial PNT2 cells. These cell lines were treated with an anti-STEAP2 pAb and their viability assessed. CRISPR/Cas9 technology was used to knockout *STEAP2* from C4-2B and LNCaP cells and viability, proliferation, migration and invasion assessed. When exposed to an anti-STEAP2 pAb, cell viability significantly decreased ($p<0.05$). When *STEAP2* was knocked out, cell viability and proliferation was significantly decreased when compared to wild-type cells ($p<0.001$). The migratory and invasive potential of knockout cells were also decreased. These data suggest that *STEAP2* has a functional role in driving aggressive prostate cancer traits and could provide a novel therapeutic target for the treatment of prostate cancer.

Doi: http://dx.doi.org/10.14715/cmb/2023.69.4.28

Introduction

Prostate cancer is the most common non-cutaneous cancer in men, accounting for 15% of all male cancer diagnoses globally (1). The lifetime risk of a man being diagnosed with prostate cancer is 1 in 8, with statistics showing that one man in the UK dies from prostate cancer every 45 minutes (2,3). When confined to the gland, prostate cancer is not usually life-threatening, as localised tumours often remain dormant and can be removed surgically through radical prostatectomies, or effectively managed through routine observations (4,5). However, once prostate cancer has metastasised, the prognosis for the patient decreases significantly, with only 30% of men with Stage 4 disease surviving for more than 5 years, compared to up to 95% of men with Stage 3 disease (6,7).

Screening is not universally available in the UK and is only recommended as an opportunistic approach in the form of PSA blood testing in men over the age of 55 presenting with prostate cancer symptoms (2,8,9). However, there is controversy over the age at which to begin screening by PSA blood tests, with the European Association of Urology recommending a baseline PSA test at 40-45 years, yet the American Urological Association suggests reserving this to over 55 years (10,11). Randomised trials of PSA screening have proven inconclusive, with one reporting that no improvement in prostate cancer mortality was observed following the screening of 420,000 men (12). As such, a PSA screening programme is not currently recommended by the National Institute for Health and Care Excellence (NICE) or supported by the World Health Organisation (WHO) (2).

Through the identification of novel biomarkers for cancer progression, further insight into the mechanisms behind prostate carcinogenesis can be developed, which may subsequently aid in the clinical management of the disease and provide a tool to improve patient stratification. Of particular interest is the six transmembrane epithelial antigen of the prostate (STEAP) family, where two of the four members (STEAP1 and STEAP2) demonstrate high expression in prostate cancer tissue when compared to normal tissue, and therefore have been suggested to have a role in prostate cancer progression (13-17).

STEAP2, also known as the six transmembrane protein of prostate 1 (STAMP1), is located on chromosome 7q21.13, contains 6 exons and 5 introns, and encodes for a 490 aa long protein with an estimated molecular weight of 56.1 kDa (13,18,23). As demonstrated in Figure 1 below, STEAP2 is predominantly located in the plasma membrane, and green-fluorescent protein (GFP) labelling revealed STEAP2 as a cell-surface protein (13). STEAP2 has been suggested to play a role in protein sorting and secretory pathways, as it shuttles to the Golgi organelle and trans-Golgi network (Figure 1; 14,19,23). *STEAP2* is significantly overexpressed in prostate cancer when compared to normal healthy tissue (16,17). Transfection with

* Corresponding author. Email: s.h.doak@swansea.ac.uk

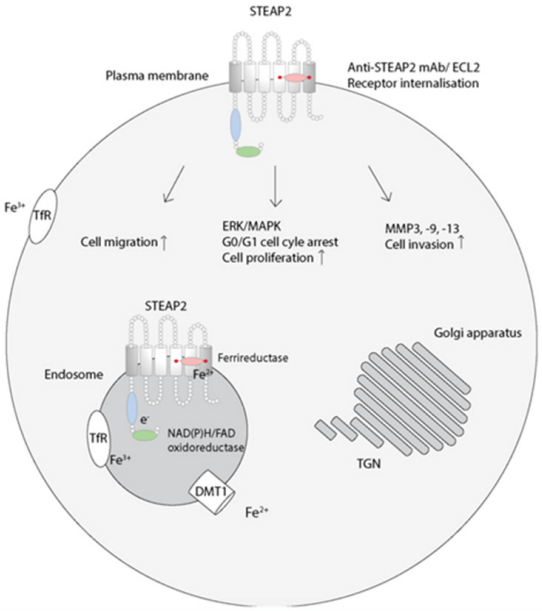

Figure 1. Cellular localisation and function of the STEAP2 protein. STEAP2 is predominantly located in the plasma membrane, the Golgi apparatus and the Trans-Golgi Network (TGN) where it is thought to partake in the secretory processing. Antibody targeting of the extracellular loop2 (ECL2) of STEAP2 results in receptor internalisation presumably to the endosomes. The transferrin-receptor (TfR) is known to uptake Fe3+ and shuttles to the endosomes, where it co-localises with STEAP2. In the endosomes, STEAP2 is presumably exhibits oxidoreductase activity by its NAD(P)H/FAD domain and uses free electrons for its ferrireductase activity to reduce Fe3+ to Fe2+. Reduced Fe2+ is then transported out of the endosomes into the cytoplasm via the dimetal-transporter1 (DMT1). Overexpressed STEAP2 protein increases cell proliferation via the ERK/MAPK signalling pathway and results in more aggressive cancer phenotypic traits such as cell migration and invasion *in-vitro* (Figure adapted by Gomes *et al.*, 2012) (19).

STEAP2 in the normal prostate cancer cell line PNT2 resulted in a more aggressive phenotype, with cells gaining an increased migratory potential (16). When *STEAP2* expression was transiently knocked down using small interfering RNA (siRNA), cancer cell migration and invasion were significantly inhibited, further suggesting a role for *STEAP2* in driving aggressive prostate cancer traits (17).

The overexpression of *STEAP2* in prostate tissue combined with the fact that prostate cancer progression is androgen dependent warrants investigation into the involvement of androgens in the regulation of *STEAP2* expression. *In vitro*, the highest *STEAP2* expression levels have been found in the androgen-sensitive lymph node metastatic prostate cancer cell line LNCaP when compared to the normal prostate epithelial cell line PNT2 (16,17). Interestingly, it has recently been shown that androgen-dependent CWR22 xenografts grown in mice, demonstrate signification regression following castration, regardless of altering the mRNA expression of *STEAP2* (23). Additionally, Wang *et al* identified that partial cell cycle arrest was found at the G_0-G_1 phase, suggesting that *STEAP2* may regulate genes involved in this stage of the cell cycle, as prostate cancer cell proliferation has been seen to increase following *STEAP2* overexpression both *in vitro* and *in vivo* (24), yet further studies are required to explore the mechanisms behind this effect.

As STEAP2 has been found to be overexpressed in prostate cancer tissues and cell lines, STEAP2 presents an attractive molecular drug target for antibody-based therapies in the treatment of advanced prostate cancer. STEAP2-knockout by CRISPR/Cas9 engineering determined the consequential effects on the capacity of prostate cancer cells to migrate and invade. Equally, the ability of an anti-STEAP2 pAb was found to reduce cell viability in a panel of prostate cancer cell lines, suggesting *STEAP2* as a potential novel therapeutic target for the treatment of prostate cancer.

This study aimed to evaluate the potential of STEAP2 as a therapeutic target through targeted STEAP2 knockout using CRISPR/Cas9 engineering, and the application of an anti-STEAP2 polyclonal antibody. Additionally, this study aimed to develop an understanding in the role of STEAP2 in driving prostate cancer progression through analysis of the migratory and invasive potential of C4-2B and LNCaP cells following STEAP2 knockout.

Materials and Methods

STEAP gene expression profiling

RNA was extracted from cells grown in androgen-depleted conditions using Trizol reagent (Thermo Fisher, USA, Cat. 15596026). First-strand total cDNA was synthesised from RNA using a Promega M-MLV Reverse Transcriptase kit (Promega, USA) following the manufacturer's instructions. Quantitative reverse transcriptase polymerase chain reaction (qRT-PCR) was carried out to determine the profiles of genes of interest. A BLAST search was performed prior to carrying out each experiment to design unique primer sequences specific to each gene of interest. Pre-validated primers for two housekeeping genes, *β-actin* (NM_001101) and *GAPDH* (NM_002046) were used in this study, the sequences of which are detailed in Table 1. All primers were reconstituted and diluted in RNAse-free water (Thermo Fisher, USA, Cat. AM9916), to a concentration of 10 mM.

PowerUp™ SYBR™ Green Master Mix (Thermo Fi-

Table 1. Sequences of primers (5' - 3') utilised in qRT-PCR experiments. Sequences of primers for the detection of *STEAP1-4,* including housekeeping genes *β-actin* and *GAPDH.*

Gene	Forward primer	Reverse primer
β-actin	CACCATTGGCAATGAGCGGTTC	AGGTCTTTGCGGATGTCCACGT
GAPDH	GTCTCCTCTGACTTCAACAGCG	ACCACCCTGTTGCTGTAGCCAA
STEAP1	CCCTTCTACTGGGCACAATACA	GCATGGCAGGAATAGTATGCTTT
STEAP2	GGTCACTGTAGGTGTGATTGG	ACCACATGATAGCCGCATCTAA
STEAP3	CTCCCCGGAGGTCATCTTTG	TCTTGCTCTGTAGGGTTGCTC
STEAP4	GGCTTTGGGAATACTTGGGTT	TGGACAAATCGGAACTCTCTCC

sher, USA, Cat. A25742) was used for the detection of genes of interest by qRT-PCR. Gene profiling was carried out using an Applied Biosystems™ QuantStudio™ 12K Flex Real-Time PCR System (Thermo Fisher, USA, Cat. 4471134).

Cycle threshold (C_T) values obtained from gene profiling were used to calculate the fold expression changes of each gene of interest, normalised to control cells. An average was taken of the raw C_T values of each experimental sample and each control sample for both genes of interest and the housekeeping genes. The relative difference in expression was calculated as $2^{-\Delta\Delta C}{}_T$ (n=3).

Targeting STEAP2 in C4-2B and LNCaP cells using CRISPR/Cas9

The non-targeting guide RNA (gRNA) control and two gRNA sequences targeting human STEAP2 were designed. Control: CGCGATAGCGCGAATATATT; STEAP2 sg1: AATATTCAAGCGCGACAAC and STEAP2 sg2: GGAATGAAATTCAACTGGC. gRNAs were cloned into a LentiCrispr v2 vector at *Bsm*BI site following the Human CRISPR Knockout Pooled Library (GeCKO v2) protocol (Addgene #1000000048). Human embryonic kidney 293T cells were co-transfected with single guide RNA containing LentiCrispr V2, packaging vector PsPAX-2 vector, and envelop vector pCMV-vsvg (Sigma, USA). The culture medium was removed and changed to RPMI-1640 complete medium after 24 h. C4-2B and LNCaP cells were transduced with lentivirus expressing control or STEAP2 gRNAs. After 48h incubation, the growth medium was changed to a selection medium containing 0.625 µg/ml and 1.25 µg/ml puromycin to maintain *STEAP2*-positive LNCaP^{KO} and C4-2B^{KO} cells respectively. Single colonies were isolated and plated into a 96-well plate and amplified once confluent. The knockout of STEAP2 was validated by Western blot analysis. Cells were pelleted and lysed in ice-cold radioimmunoprecipitation assay buffer (RIPA; Sigma Aldrich, USA, Cat. R0278). Protein concentration was determined by Bradford assay (BioRad, USA, Cat. 5000002). Equal amounts of total cell lysates were resolved by SDS-PAGE, transferred to a nitrocellulose membrane and then immunoblotted with antibodies against STEAP2 or GAPDH, followed by HRP-conjugated secondary antibodies. Blots were then visualised by enhanced chemiluminescence using The ChemiDocXRS+ (BioRad, USA) for image acquisition, and ImageLab software, Version 6.0.1 for analysis.

Cell viability

To assess cell proliferation in STEAP2-knockout cells, the commercial resazurin-based dye alamarBlue assay (BioRad, UK, Cat. BUF012A), was performed as per manufactures instructions. Proliferation was assessed in LNCaP and C4-2B knockout cells and compared to that of wild-type cells. Viability assays were conducted in triplicate.

Migration assay

After C4-2B and LNCaP cells had reached ~80% confluency, the medium was replaced for 24 h with serum-free DMEM and RPMI-1640 medium respectively. Cells were trypsinised, resuspended and adjusted to a desired cell concentration. One silicone cell culture insert (IBIDI, Germany, Cat. 80209) was placed in the centre of a well of a 12-well plate, and 70 µl cell suspension was added per chamber. LNCaP^{WT} and LNCaP^{KO} cells were incubated for 72 h prior to the removal of the silicone inserts, whilst C4-2B^{WT} and C4-2B^{KO} cells were incubated for 48 h. Media and inserts were removed, and cells were washed with PBS to remove cell debris before fresh media was applied. The time taken to close the gap created was monitored using an inverted light microscope (Invitrogen, EVOS XL Core, USA). Media was replaced every 3 days. The migration assay was conducted in triplicate.

Invasion assay

48 h prior to each invasion assay, cells were harvested and seeded in 6-well plates at a density of 3 x 105 cells/ml and left to adhere to standard cell culture conditions. Cultures were serum starved in serum-free media (SFM) for 24 hours. Prior to seeding cells, 20 µl of growth factor reduced (GFR) Matrigel (1:5 dilution/SFM; Corning) was applied to the Transwell insert and polymerised for 1 hour in standard cell culture conditions. Cells were harvested with trypsin and adjusted to a desired seeding density in a volume of 250 µl SFM. Prior to the addition of cells, 600 µl of serum-containing media was added to the lower chamber. LNCaP^{WT} and LNCaP^{KO} cells were incubated for 72 h prior to staining, whilst C4-2B^{WT} and C4-2B^{KO} cells were incubated for 48 h in standard cell culture conditions to allow for cell invasion to occur. Cell invasion was quantified through staining with crystal violet. Invaded cells were fixed with 100% methanol for 15 minutes at room temperature and allowed to air dry. They were stained with a crystal violet staining mixture (0.5% crystal violet in 20% methanol) for 30 minutes to allow visualisation of cells. The non-invaded cells on the upper surface of the Transwell insert were removed with a cotton swab moistened in media. The inserts were washed in purified water and left to air dry for 1 hour. Invaded cells were visualised using a standard light microscope at 10x magnification (Invitrogen, EVOS XL Core, USA). Images were taken of different planes of each insert and the invasion assay was conducted in triplicate.

Targeting STEAP2 with anti-STEAP2 antibodies

A commercially available anti-STEAP2 polyclonal antibody (stock concentration 1 mg/ml) which targets the third extracellular loop (ECL) of STEAP2 was used in this study (Aviva Systems Biology, OASG06901). Monolayers of prostate cancer cells were cultured in 96-well plates. Cells were exposed to anti-STEAP2 antibodies. To determine cell viability following exposure to anti-STEAP2 antibodies, the MTT cell viability assay (Sigma Aldrich, UK, #T9281) was used Absorbance was read at A = 570 nm using a fluorescence plate reader (POLARstar, BMG Labtech, UK) and viability calculated as a percentage of the untreated control. The cell viability experiments were conducted in triplicate.

Statistical analysis

Statistical analysis was performed using GraphPad Prism version 8 for iOS, using the one-way ANOVA *post-hoc* Dunnett test. Data were considered statistically significant when a p-value of < 0.05 (*), p-value < 0.01 (**) or p- value of < 0.001 (***) or p-value < 0.0001 (****) was obtained, which were annotated within the respective figures.

Results

Expression of STEAP family members in prostate cancer cells

The gene expression profile of all four members of the STEAP family was evaluated in a panel of prostate cancer cells to establish any variation in transcriptional levels associated with prostate cancer epithelial cells. Two AR-independent prostate cancer cell lines (PC3 and DU145) and two AR-sensitive prostate cancer cell lines (LNCaP and C4-2B) were selected to assess whether there was any correlation between AR sensitivity and STEAP expression. In addition, the normal prostate epithelial cell line PNT2 was used for comparison.

STEAP2 was found to have the highest level of expression in three of the four prostate cancer cell lines (LNCaP, PC3 and C4-2B) screened, with significantly higher levels of *STEAP2* observed in the androgen-sensitive cell lines, LNCaP and C4-2B, which exhibited 264.7-fold and 53.5-fold higher expression than the normal prostate epithelial PNT2 cell line, respectively (Figure 2a). *STEAP1*, *STEAP3* and *STEAP4* were all found to have lower levels of expression in all prostate cancer cell lines when compared to PNT2 cells, except for *STEAP1* in LNCaP cells (31.7-fold increase) (Figure 2a). To determine whether the increase in *STEAP2* mRNA expression translated to a protein level, Western blots were carried out on the two cell lines with the highest mRNA expression: C4-2B and LNCaP (Figure 2b).

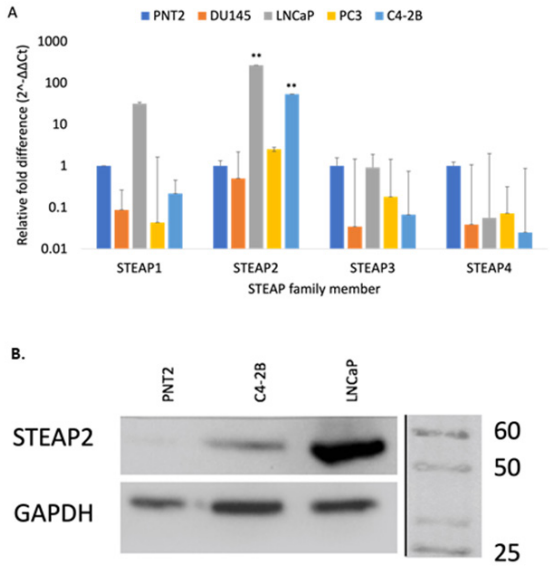

Figure 2. *STEAP1-4* gene and protein expression in human prostate cancer cell lines. (A) qRT-PCR of *STEAP1-4* to establish gene expression levels in four human prostate cancer cell lines. Gene expression fold differences were normalised to the normal prostate epithelial cell line PNT2, which was defined as having an expression value of 1.0. GAPDH was used as the housekeeping gene. An ANOVA post-hoc Dunnett test was performed for statistical analysis. Error bars denote S.E.M. p-value < 0.05 (*), p-value < 0.01 (**). (N = 3). **(B)** Protein lysates were taken from PNT2, C4-2B and LNCaP cells. STEAP2: approx. 56 kDa; GAPDH: approx. 37 kDa. (Loading control = GAPDH, Black lines represent where the western blot image has been edited for clarity).

Cell proliferation, migration and invasion following STEAP2 knockout using CRISPR/Cas9.

CRISPR/Cas9 technology was optimised for successful targeted STEAP2 knockout in LNCaP and C4- 2B prostate cancer cells *in vitro*. LNCaP and C4-2B cells were selected due to their high baseline gene expression of STEAP2 (Figure 2b). Once successful STEAP2 knockout had been achieved and confirmed by western blot (see Supplementary Figure 1), these modified cells ($LNCaP^{KO}$ and $C4\text{-}2B^{KO}$), were utilised to evaluate its impact on cell viability, proliferation, migration, and invasion.

To determine the consequence of the CRISPR/Cas9 knockout of STEAP2 in LNCaP and C4-2B cells on cell proliferation, the alamarBlue cell proliferation assay was performed. The percentage of proliferating cells was normalised to cells on day 1 to determine the difference in proliferation rate over time. In $LNCaP^{KO}$ cells, the percentage of proliferating cells was significantly reduced on day 3 (-48%, $p < 0.05$; Figure 3a), after which the experiment was ended due to excessive cell death. The percentage of proliferating $C4\text{-}2B^{KO}$ cells was also consistently and significantly reduced across all 5 days and was lowest on day 5 (-53%, $p < 0.0001$; Figure 3b). Based on these data, it can be suggested that *STEAP2* knockout significantly reduces the proliferative capacity of androgen-sensitive prostate cancer cell lines.

To further evaluate the potential of CRISPR/Cas9 knockout of *STEAP2* on reducing aggressive characteristics of LNCaP and C4-2B cells, the cell migration assay was carried out. In LNCaP cells, whilst the wound gap was not completely closed in wild-type cells by day 5 (Figure 4b), *STEAP2* knockout completely inhibited the migration of $LNCaP^{KO}$ cells (Figure 4b). In C4-2B cells, the wound gap had entirely closed between days 3 and 5 in $C4\text{-}2B^{WT}$ cells (Figure 4c), suggesting that they migrate at a faster rate than $LNCaP^{WT}$ cells. In contrast, in $C4\text{-}2B^{KO}$ cells,

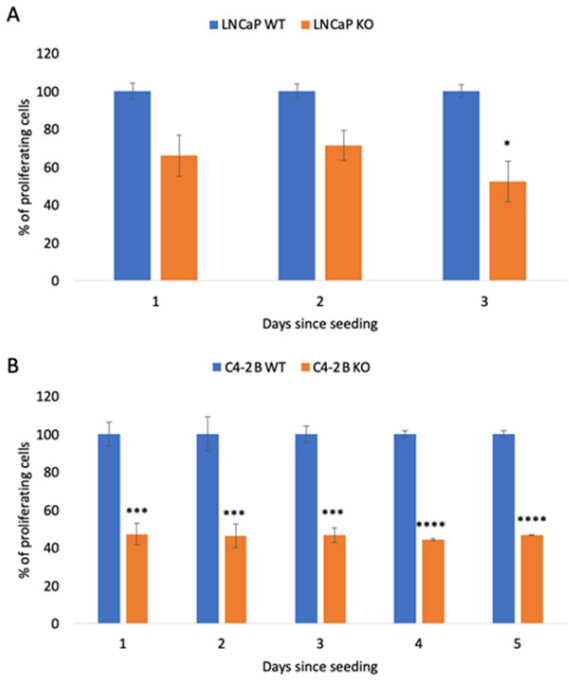

Figure 3. *STEAP2* knockout significantly reduces cell proliferation. Quantification by alamarBlue assay of the percentage of proliferating cells in $LNCaP^{KO}$ (A) and $C4\text{-}2B^{KO}$ (B) cells in comparison to their wild-type counterparts. An ANOVA post-hoc Dunnett test was performed for statistical analysis. Error bars denote S.E.M. p-value < 0.05 (*), p-value < 0.01 (**), p-value < 0.001 (***), p-value < 0.0001 (****) (N = 3).

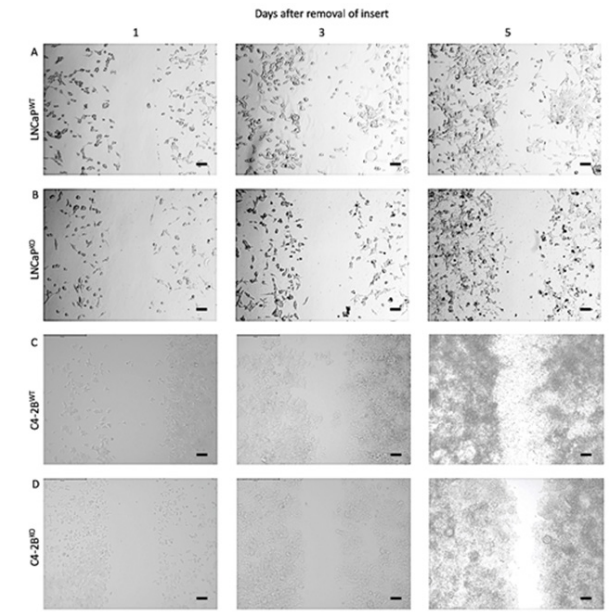

Figure 4. *STEAP2* knockout decreases the migratory potential of LNCaP and C4-2B cells. Each panel represents A) LNCaP^{WT}, B) LNCaP^{KO} cells and C) C4-2B^{WT}, D) C4-2B^{KO} cells. Time points at which the images were taken: 0 days, 3 days and 6 days. Wild-type LNCaP and C4-2B cells were used as positive controls. Images were acquired using an inverted light microscope with a 10x objective (Invitrogen, EVOS XL Core, USA). Scale bar = 100 µm. (Illustrated are representative images; the experiment was however conducted in triplicate with biological replicates, N = 3).

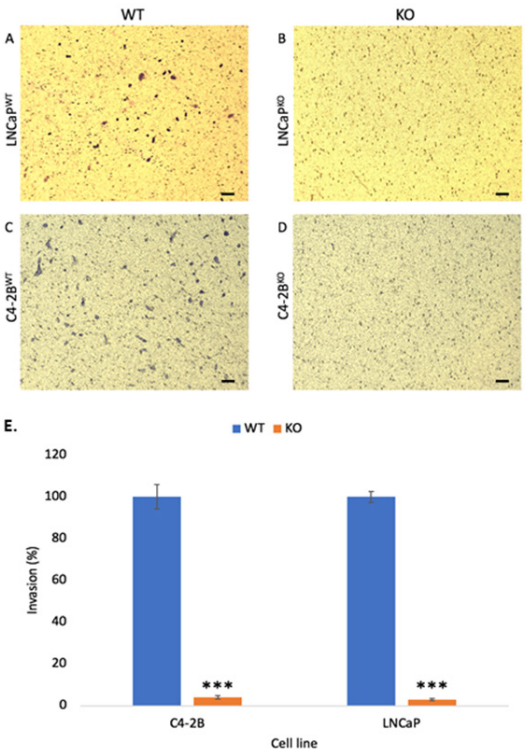

Figure 5. *STEAP2* knockout reduces the invasive potential of LNCaP and C4-2B cells. Images of stained cells were taken to give a visual representation of invasion. Each panel represents A) LNCaP^{WT}, B) LNCaP^{KO} cells and C) C4-2B^{WT}, D) C4-2B^{KO} cells. LNCaP^{WT} and C4-2B^{WT} cells show invasive potential. STEAP2 knockout in LNCaP^{KO} and C4-2B^{KO} cells reduces invasive capacity. Invaded cells were stained with crystal violet. Images were taken 48 h (C4-2B) and 72 h (LNCaP) after seeding. E) The number of stained cells that had invaded through the Transwell insert was counted and calculated as a percentage of the wild-type control. An unpaired t-test was performed for statistical analysis. Error bars denote S.E.M. p-value < 0.05 (*), p-value < 0.01 (**), p-value < 0.001 (***), p-value < 0.0001 (****). Images were taken with an inverted light microscope at a 10x objective (Invitrogen, EVOS XL Core, USA). Scale bar = 100 µm. The experiment was conducted in triplicate with biological replicates, N = 3.

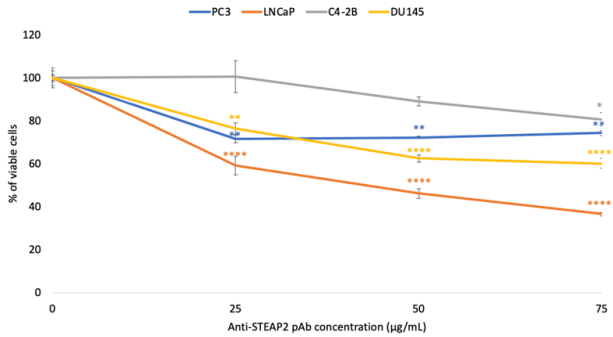

Figure 6. Effect of anti-STEAP2 pAb on prostate cancer cell viability. PC3, LNCaP, C4-2B and DU145 prostate cancer cells were treated with increasing concentrations of anti-STEAP2 pAb. After 24 h treatment, cell viability was assessed by the MTT assay. An ANOVA post-hoc Dunnett test was performed for statistical analysis. Error bars denote S.E.M. p-value < 0.01 (**), p-value < 0.001 (***), p-value < 0.0001 (****) (N = 3).

inhibition in cell migration was still observed on day 5 as the wound gap remained fully open (Figure 4d). These data indicate that *STEAP2* knockout leads to substantial inhibition of the migratory capacity of both LNCaP^{KO} and C4-2B^{KO} cells (Figure 4).

A cell invasion assay was performed to evaluate whether targeted knockout of *STEAP2* using CRISPR/Cas9 engineering inhibited cancer cell invasion. Cells were grown in the top layer of an insert, and as such only those with invasive potential were capable of crossing the Matrigel barrier. The invasive potential of LNCaP and C4-2B cells is significantly inhibited with *STEAP2* knockout with only 3.0% and 4.1% of LNCaP^{KO} and C4-2B^{KO} cells respectively, invading through the ECM as compared to the equivalent wild-type cells ($p < 0.001$; Figure 5e). These data, along with the results presented in Figures 3 & 4 which showed that *STEAP2* knockout decreases cellular proliferation and migration, suggest that *STEAP2* knockout substantially reduces aggressive cancer traits in LNCaP and C4-2B cells (Figure 5).

Targeting STEAP2 with anti-STEAP2 antibodies

Having demonstrated that the effective knockout of STEAP2 using a CRISPR/Cas9 approach was effective at reducing associated cancer-related cell responses, we explored whether a similar effect could be achieved by targeting STEAP2 using an antibody-based approach. The ability of a commercially available anti-STEAP2 polyclonal antibody to induce cell death in prostate cancer cells, was assessed using an MTT cell viability assay. Cells were exposed to three different doses of anti-STEAP2 polyclonal antibody: 25, 50 and 75 µg/ml for 24 h before viability assays were conducted (Figure 6). All doses induced significant reductions in the percentage of viable cells in PC3, DU145 and LNCaP cells (Figure 6). The largest reduction in the percentage of viable cells was observed in LNCaP cells at the highest pAb dose of 75 µg/ml (-63.4%, $p < 0.0001$; Figure 6). In C4-2B cells, only the highest dose of

75 µg/ml induced a significant reduction in cell viability (-19.2%, $p < 0.05$); Figure 6). Interestingly, in PC3 cells, reduction in the number of viable cells did not occur in a dose-dependent manner, with an initial 28.5% decrease in the percentage of viable cells when treated with 25 g/ml anti-STEAP2 pAb, which was not increased further despite further increases in doses ($p < 0.01$; Figure 6). These data suggest that further increasing the dose in PC3 cells is not warranted as no further biological effect was observed. Overall, these data revealed that 75 µg/ml anti-STEAP2 pAb substantially decreased the viability of all four prostate cancer cell lines.

Discussion

STEAP2, a cell surface protein that functions as a metalloreductase, is highly expressed in prostate cancer when compared to normal tissue and is known to contribute to disease progression by modulating aggressive prostate cancer traits such as cell migration and invasion *in vitro* (13-15). This study aimed to determine the effects of targeting STEAP2 with anti-STEAP2 polyclonal antibodies, and CRISPR/Cas9 knockout, on aggressive prostate cancer traits, with a view to the use of STEAP2 as a potential therapeutic target. To do so, targeted *STEAP2* knockout was established to determine if it could reduce invasive traits in androgen-sensitive prostate cancer cells. Furthermore, the ability of a commercially available anti-STEAP2 pAb on reducing cell viability in a panel of prostate cancer cell lines was assessed.

CRISPR/Cas9 technology can induce complete gene knockout, as opposed to the transient gene knockdown offered by siRNA silencing (37,38). siRNA silencing has previously been used to target *STEAP2 in vitro*, however only a 50% reduction in protein expression was reported, highlighting the need for a more efficient genome engineering tool (17). The expression of *STEAP2* and other family members was evaluated in a panel of prostate cancer cells (Figure 2). Based on the gene expression profiles, LNCaP and C4-2B cells were selected for *STEAP2* knockout, as their high *STEAP2* gene expression levels were mirrored when evaluating STEAP2 protein levels, which for LNCaP, correlates with observations reported in previous studies (Figure 2a; (16)).

Here, CRISPR/Cas9 targeted *STEAP2* knockout significantly reduced the proliferation of $LNCaP^{KO}$ and $C4\text{-}2B^{KO}$, which was sustained over a 3- and 5-day period, respectively (Figure 3). The role of *STEAP2* in cell proliferation has previously been explored by Wang *et al*., who found that when *STEAP2* was overexpressed in COS-7 normal monkey kidney fibroblast cells, an increase in cell proliferation rate occurred (24). In the same study, *STEAP2* was ectopically expressed in DU145 prostate cancer cells, which resulted in ERK activation in response to EGF, the expression of which was increased in response to *STEAP2* (24). Once ERK becomes phosphorylated, a variety of transcription factors become activated upon the translocation of ERK into the nucleus, including AP-1, which has canonical sequences with matrix metalloproteinases (MMPs) -1, -3, -7, -9, -11 and -13 (39,40). The role of *STEAP2* in cellular proliferation has previously been found to be coordinated through the activation of the ERK pathway, which when activated by *STEAP2* induces this partial cell cycle arrest in the G_0-G_1 phase of the cell cycle in cancer cells, and in turn, increases cell proliferation and tumour progression (19,24).

When the expression of *STEAP2* has been knocked down by the presence of *STEAP2* siRNA, the proliferation of LNCaP cells was found to significantly decrease, yet no changes in cellular morphology were observed (24). Studies into the changes in the distribution of the cell cycle of LNCaP cells transfected with *STEAP2* siRNA found that there was a significant increase in the percentage of cells in the G_1 phase, which corroborated with a decrease in cells in the S phase, suggesting that loss of *STEAP2* results in a partial cell cycle arrest in G_0-G_1 (24). When monitoring the proliferation of cells transfected with *STEAP2* siRNA using the proliferative marker Ki67, Wang *et al*., found that Ki67 was significantly downregulated by day 4 in LNCaP cells transfected with *STEAP2* siRNA, further confirming the proliferative influence of *STEAP2* expression. Therefore, in this study, an absence of *STEAP2* expression may have led to a decrease in cell proliferation as the ERK pathway would not become activated by *STEAP2*, and in turn, the partial arrest at G_0-G_1 observed in previous studies may have occurred (24). The results in this study further confirm that *STEAP2* inhibition significantly reduces cell proliferation, as demonstrated by previous studies (17,24). This reduction in proliferation may be the result of an inability to progress through the G_0-G_1 phase of the cell cycle (24). However, the exact mechanisms by which *STEAP2* knockout reduces proliferation remain to be fully elucidated.

An essential mechanism in the progression of prostate cancer is the ability of cells to migrate to distant sites to form metastases (41). *STEAP2* has previously been hypothesised to be involved in promoting cancer cell migration, thus enhancing prostate cancer progression (16, 17). Here we evaluated whether complete gene knockout of *STEAP2* from prostate cancer cells using CRISPR/Cas9 technology would significantly inhibit cancer cell migration. Indeed, the data generated through use of the proliferation assay demonstrated that *STEAP2* knockout significantly reduced proliferation in both cell lines (Figure 3). Furthermore, it was found that the migration of *STEAP2* knockout cells was impaired in comparison to their wild-type counterparts (Figure 4). These results confirm those of previous studies which indicate that *STEAP2* plays a role in the migration of prostate cancer cells (16, 17).

One of the principal ways of blocking cancer progression is to inhibit cell motility, and subsequently reduce cell migration and invasion (43). When downregulated, another member of the *STEAP* family, *STEAP4*, has been found to significantly increase ROS via iron reductase activity (44,45). Whilst ROS increases are often associated with an increase in mutations and disease progression, the induction of excessive ROS activity in prostate cancer cells has been found to reduce tumour cell motility and metastasis through the inhibition of epithelial-mesenchymal transitions (46). Apoptosis was also found to increase in response to elevated ROS, as a result of caspase-3 and -9 activation and cytochrome-c release (46). Similar to *STEAP4, STEAP2* also contains an N-terminal oxidoreductase domain with a nicotinamide adenine di-nucleotide phosphate (NADPH) binding motif, which can serve as an electron donor for transmembrane electron transport of iron and copper (14,42,45). An increase in iron uptake has been found to increase ROS and promote carcinogenesis,

suggesting targeting iron metabolism may be a potential therapeutic approach in the treatment of some cancers (47,48). Therefore, it could be suggested that the decrease in migration observed here could be the result of *STEAP2* knockout inducing an increase in ROS activity through impaired iron reductase activity. However, as this connection between ROS and *STEAP2* remains unclear, further studies would be warranted to determine the intercellular localisation of ROS in *STEAP2*-knockout cells compared to their wild-type counterparts (46).

As with migratory capacity, the invasion potential of PC3 cells has been found to substantially decrease following the gene knock-down of *STEAP2* using siRNA technology (17). Additionally, when the normal prostate epithelial cell line PNT2 has previously been transfected with a *STEAP2* plasmid to overexpress the gene, cells gained the ability to invade through the extracellular matrix (16). Our data suggest that *STEAP2* may play a role in the invasive potential of LNCaP and C4-2B cells, which was significantly reduced in both cell lines by 97.0% and 95.9% respectively (Figure 5).

LNCaP cells were found to have the highest naturally occurring levels of *STEAP2* expression (Figure 2), and in this study, LNCaP cells were most susceptible to anti-STEAP2 pAb-induced cell death (Figure 6). Previously STEAP2-knockdown has also been found to increase the sensitivity of LNCaP cells to tumour necrosis factor-related apoptosis-inducing ligand (TRAIL)-induced apoptosis (24). Other drugs that trigger TRAIL-induced apoptosis in prostate cancer include anthracycline doxorubicin (27,28). TRAIL-induced apoptosis is often the result of caspase-3, -6 and -8 mediated cell death (25,28-30). Caspase-8 mediated apoptotic cell death has also been linked to DISC formation in response to TRAIL signalling receptors triggering the extrinsic pathway of apoptosis (29). Furthermore, targeting other members of the STEAP family with mAbs has been found to trigger caspase-dependent apoptosis (31-33).

Upon cell death, the apoptotic cascade is triggered, yet it is unclear which of the apoptotic pathways STEAP2 is involved in (24). As STEAP2 is localised to the cell membrane, it has been suggested that the extrinsic apoptosis pathway may be affected by STEAP2 (24). During the extrinsic apoptosis pathway, the signalling of cell surface receptors initiates a cascade, ultimately resulting in cell death through the formation of the death-inducing signalling complex (DISC) (24,29). STEAP2 may exert its effect on this pathway by decreasing the stability of the DISC (24). It has also been suggested that STEAP2 may play a role in the intrinsic apoptosis pathway, as cells with STEAP2-knockdown have been found to undergo apoptosis in the absence of induction of the extrinsic apoptosis pathway through transcription factors (24,25). STEAP2 is localised to the Golgi, and as such may interact with and affect the function of anti-apoptotic proteins such as the Golgi anti-apoptotic protein, which has been found to inhibit apoptosis through modulation of intracellular calcium fluxes (26). The endocytic trafficking of cell surface receptors that influence receptor signalling, essential for cell growth or apoptosis, may also be influenced by STEAP2 (24).

Whilst anti-STEAP2 monoclonal antibodies have not yet been widely studied, targeting other STEAP family members has induced promising tumour growth inhibition both *in vitro* and *in vivo* (34,35). Two anti-STEAP1 monoclonal antibodies specific to STEAP1 extracellular loops successfully inhibited STEAP1-mediated intercellular communication and transport *in vitro*, and significantly reduced the growth of prostate cancer xenografts *in vivo* (35). The ability of anti-STEAP2 antibodies to inhibit cell growth warrants further investigations into its effects on intercellular communication, which may provide a link between STEAP2 and intercellular ion transport. Like STEAP1, STEAP2 also contains a heme-binding domain known as the ACRATA (20). This ACRATA domain is also present in a structurally related family which includes STEAP family members, the bacterial NOX family, and the oxidoreductase family YedZ (19,20). Electron transfer may be supported through this heme-binding function, which has been found to affect cell growth and metabolism in NOX proteins, and electron transport across membranes in both NOX and STEAP proteins (21,22). It would therefore be of interest in the future to evaluate the role of the ACRATA domain when cell death is induced in response to anti-STEAP2 antibody exposure.

Together, the data presented here provide evidence that *STEAP2* plays an important role in the progression of androgen-sensitive prostate cancer cells as the ability of both LNCaP and C4-2B to proliferate, migrate and invade was significantly decreased when *STEAP2* was knocked out. Whilst the key mechanism behind how *STEAP2* knockout inhibits cell migration remains unknown, the data presented here imply that *STEAP2* could provide a novel therapeutic target for inhibiting prostate cancer migration and metastasis.

STEAP2 shows promise as a potential novel therapeutic target due to its overexpression being specific to prostate cancer tissues, coupled with a low expression profile in other normal tissues. CRISPR/Cas9 technology was successfully optimised and developed to generate stable STEAP2-knockout in AR-sensitive LNCaP and C4-2B cells *in vitro*. This knockout further implicates *STEAP2* as a potential therapeutic target as LNCaP^{KO} and C4-2B^{KO} exhibited reduced proliferation, migration and invasive potential compared to their wild-type counterparts. Mono- and polyclonal antibodies have shown potential in the treatment of various cancers, yet their use in prostate cancer is limited. The anti-STEAP2 polyclonal antibody applied within this study target the ECL3 of STEAP2 showed value in reducing prostate cancer cell viability and proliferation *in vitro*. These findings highlight the therapeutic benefit of antibody-based therapeutics targeting the ECL3 of STEAP2 based on the ability of the anti-STEAP2 pAb to reduce cell viability in prostate cancer cells. The *in vitro* findings of this study, therefore, support *STEAP2* as a viable therapeutic target for reducing aggressive prostate cancer traits, either as an antibody per se or potentially as an antibody-drug conjugate.

Author Contributions

Conceptualization, L.A.J. and S.H.D.; methodology and investigation, L.A.J., A.N. and S.H.D.; formal analysis, L.A.J.; resources, G.J.J., R.S.C. and S.H.D.; data curation, L.A.J., A.N. and S.B.; writing—original draft preparation, L.A.J.; writing—review and editing, L.A.J., G.E.C., A.N., S.B., G.J.J., R.S.C. and S.H.D.; supervision, G.J.J, R.S.C. and S.H.D.; project administration, S.H.D.; funding acquisition, S.H.D. All authors have read and agreed to the pu-

blished version of the manuscript.

Funding
This research received no external funding.

Data Availability Statement
Data will be made freely available upon request to the corresponding author.

Acknowledgments
We would like to thank Dr Shu-Hsia Chen and colleagues Hui-Ju Lee, Yi-Ling Wang and Kyeongah Kang at the Center for Immune Therapy Research, Houston Methodist Research Institute for their help and expertise in generating CRISPR/Cas9 knockout cell lines. We would also like to thank Dr Bin He for providing the prostate cancer cell lines used at the Cancer Centre, Houston Methodist Research Institute.

Conflicts of Interest
The authors declare no conflict of interest.

References

1. Ferlay J, Soerjomataram I, Dikshit R, Eser S, Mathers C, Rebelo M, *et al*. Cancer incidence and mortality worldwide: sources, methods and major patterns in GLOBOCAN 2012. Int J Cancer, 2015; 136:E359-86.
2. Nelson AW, Shah N. Prostate cancer. Surgery (Oxford), 2019; 37:500-507.
3. Prostate Cancer UK. (2020). Statistics.
4. Moschini M, Spahn M, Mattei A, Cheville J, Karnes RJ. (2016). Incorporation of tissue-based genomic biomarkers into localized prostate cancer clinics. BMC Med, 2016; 14:67.
5. Wilt TJ, Brawer MK, Jones KM, Barry M, Aronson WJ, Fox S, *et al*. Radical prostatectomy versus observation for localized prostate cancer. New Eng J Med, 2012; 367:203-213.
6. Cancer Research UK. (2019). Cancer Statistics.
7. National Comprehensive Cancer Network. (2018). *Prostate Cancer.*
8. Basch E, Oliver TK, Vickers A, Thompson I, Kantoff P, Parnes H et al (2012). Screening for prostate cancer with prostate-specific antigen testing: American Society of Clinical Oncology Provisional Clinical Opinion. J Clin Oncol, 2012; 30:020-3025.
9. Lee DJ, Mallin K, Graves AJ, Chang SS, Penson DF, Resnick MJ *et al*. Recent changes in prostate cancer screening practices and prostate cancer epidemiology. J Urol, 2017; 198:1230-1240.
10. Cabarkapa S, Perera M, McGrath S, Lawrentschuk N. Prostate cancer screening with prostate-specific antigen: A guide to the guidelines. Prostate Int, 2016; 4:125-129.
11. Carter HB, Albertsen PC, Barry MJ, Etzioni R, Freedland SJ, Greene KL *et al*. Early detection of prostate cancer: AUA Guideline. J Urol, 2013; 190:419-426.
12. Martin RM, Donovan JL, Turner EL, Metcalfe C. Young GJ, Walsh EI, *et al*. Effect of a low-intensity PSA-based screening intervention on prostate cancer mortality: the CAP randomized clinical trial. Jama, 2018; 319:883-895.
13. Porkka KP, Helenius MA, Visakorpi T. Cloning and characterization of a novel six-transmembrane protein STEAP2, expressed in normal and malignant prostate. Lab Invest, 2002; 82:1573-1582.
14. Grunewald TG, Bach H, Cossarizza A, Matsumoto I. The STEAP protein family: versatile oxidoreductases and targets for cancer immunotherapy with overlapping and distinct cellular functions. Biol Cell, 2012; 104:641-657.
15. Sikkeland J, Sheng X, Jin Y, Saatcioglu F. STAMPing at the crossroads of normal physiology and disease states. Mol Cell Endocrinol, 2016; 425:26-36.
16. Whiteland H, Spencer-Harty S, Morgan C, Kynaston H, Thomas DH, Bose P *et al*. A role for STEAP2 in prostate cancer progression. Clin Exp Metastasis, 2014;31:909-920.
17. Burnell SE, Spencer-Harty S, Howarth S, Bodger O, Kynaston H, Morgan C, *et al*. STEAP2 knockdown reduces the invasive potential of prostate cancer cells. Sci Rep, 2018; 8:1-12.
18. Ohgami RS, Campagna DR, McDonald A, Fleming MD. The Steap proteins are metalloreductases. Blood, 2006;108:1388-1394.
19. Gomes IM, Maia CJ, Santos CR. STEAP proteins: from structure to applications in cancer therapy. Mol Cancer Res, 2012; 10:573-587.
20. Sanchez-Pulido L, Rojas AM, Valencia A, Martinez-A C, Andrade MA.. ACRATA: a novel electron transfer domain associated to apoptosis and cancer. *BMC Cancer*, 2004; *4*:98.
21. Oosterheert W, Reis J, Gros P, Mattevi A. An Elegant Four-Helical Fold in NOX and STEAP Enzymes Facilitates Electron Transport across Biomembranes—Similar Vehicle, Different Destination. Accounts Chem Res, 2020; 53:1969-1980.
22. Yamada T, Hiraoka Y, Gupta TKD, Chakrabarty AM. Regulation of mammalian cell growth and death by bacterial redox proteins: relevance to ecology and cancer therapy. Cell Cycle, 2004; 3:750-753.
23. Korkmaz KS, Elbi C, Korkmaz CG, Loda M, Hager GL, Saatcioglu F. Molecular cloning and characterization of STAMP1, a highly prostate-specific six transmembrane protein that is overexpressed in prostate cancer. *J Biol Chem, 2002; 277:36689-36696.*
24. Wang L, Jin Y, Arnoldussen YJ, Jonson I, Qu S, Mælandsmo GM*, et al*. STAMP1 is both a proliferative and an antiapoptotic factor in prostate cancer. Cancer Res, 2010; 70:5818-5828.
25. Nguyen-Chi, A. (2020). *Design and evaluation of anti-STEAP2 antibodies to treat aggressive prostate cancer* (PhD). Swansea University.
26. Sayers TJ. Targeting the extrinsic apoptosis signalling pathway for cancer therapy. Cancer Immunol Immunother, 2011; 60:1173-1180.
27. De Mattia F, Gubser C, Van Dommelen MM, Visch HJ, Distelmaier F, Postigo A, *et al*. Human Golgi antiapoptotic protein modulates intracellular calcium fluxes. Mol Biol Cell, 2009; 20:3638-3645.
28. Kelly MM, Hoel BD, Voelkel-Johnson C. Doxorubicin pretreatment sensitizes prostate cancer cell lines to TRAIL induced apoptosis which correlates with the loss of c-FLIP expression. Cancer Biol Ther, 2002; 1:520-527.
29. Wu XX, Kakehi Y, Mizutani Y, Kamoto T, Kinoshita H, Isogawa YOSHIAKI *et al*. Doxorubicin enhances TRAIL-induced apoptosis in prostate cancer. Int J Oncol, 2002; 20: 949-954.
30. Dickens LS, Boyd RS, Jukes-Jones R, Hughes MA, Robinson GL, Fairall L, *et al*. A death effector domain chain DISC model reveals a crucial role for caspase-8 chain assembly in mediating apoptotic cell death. Mol Cell, 2012; 47:291-305.
31. Nimmanapalli R, Perkins CL, Orlando M, O'Bryan E, Nguyen D, Bhalla KN. Pretreatment with paclitaxel enhances apo-2 ligand/tumor necrosis factor-related apoptosis-inducing ligand-induced apoptosis of prostate cancer cells by inducing death receptors 4 and 5 protein levels. Cancer Res, 2001; 61:759-763.
32. Qin DN, Kou CZ, Ni YH, Zhang CM, Zhu JG, Zhu C, *et al*. (2010). Monoclonal antibody to the six-transmembrane epithelial antigen of prostate 4 promotes apoptosis and inhibits proliferation and glucose uptake in human adipocytes. Int J Mol Med, 2010; 26:803-811.

33. Qin DN, Zhu JG, Ji CB, Kou CZ, Zhu GZ, Zhang CM, *et al*. Monoclonal antibody to six transmembrane epithelial antigen of prostate-4 influences insulin sensitivity by attenuating phosphorylation of P13K (P85) and Akt: possible mitochondrial mechanism. J Bioenergetics Biomemb, 2011; 43:247-255.
34. Tanaka Y, Matsumoto I, Iwanami K, Inoue A, Minami R, Umeda N, *et al*. Six-transmembrane epithelial antigen of prostate4 (STEAP4) is a tumor necrosis factor alpha-induced protein that regulates IL-6, IL-8, and cell proliferation in synovium from patients with rheumatoid arthritis. Modern Rheumatol, 2012; 22:128-136.
35. Barroca-Ferreira J, Pais JP, Santos MM, Goncalves AM, Gomes IM, Sousa I, *et al*. Targeting STEAP1 protein in human cancer: current trends and future challenges. Curr Cancer Drug Targets, 2018; 18:222-230.
36. Challita-Eid PM, Morrison K, Etessami S, An Z, Morrison KJ, Perez-Villar JJ *et al*. Monoclonal antibodies to six-transmembrane epithelial antigen of the prostate-1 inhibit intercellular communication in vitro and growth of human tumor xenografts in vivo. Cancer Res, 2007; 67:5798-5805.
37. Boutros M, Ahringer J. The art and design of genetic screens: RNA interference. Nature Rev Gen, 2008; 9:554-566.
38. Tuladhar R, Yeu Y, Piazza JT, Tan Z, Clemenceau JR, Wu X, *et al*. CRISPR-Cas9-based mutagenesis frequently provokes on-target mRNA misregulation. Nature Comm, 2019; 10:1-10.
39. Dhillon AS, Hagan S, Rath O, Kolch W. MAP kinase signalling pathways in cancer. Oncogene, 2007; 26:3279-3290.
40. Gong Y, Chippada-Venkata UD, Oh WK. Roles of matrix metalloproteinases and their natural inhibitors in prostate cancer progression. Cancers, 2014; 6:1298-1327.
41. Rycaj K, Tang DG. Molecular determinants of prostate cancer metastasis. Oncotarget, 2017; 8:88211.
42. Knutson MD. Steap proteins: implications for iron and copper metabolism. Nutrition Rev, 2007; 65:335-340.
43. Palmer TD, Ashby WJ, Lewis JD, Zijlstra A. Targeting tumor cell motility to prevent metastasis. *Ad Drug Delivery Rev*, 2011; *63*:568-581.
44. Jin Y, Wang L, Qu S, Sheng X, Kristian A, Mælandsmo GM, *et al*. STAMP2 increases oxidative stress and is critical for prostate cancer. EMBO Mol Med, 2015; 7:315-331.
45. Scarl RT, Lawrence CM, Gordon HM, Nunemaker CS. STEAP4: its emerging role in metabolism and homeostasis of cellular iron and copper. J Endocrinol, 2017; 234:R123-R134.
46. Das TP, Suman S, Damodaran C. Induction of reactive oxygen species generation inhibits epithelial–mesenchymal transition and promotes growth arrest in prostate cancer cells. Mol Carcinogen, 2014; 53:537-547.
47. Bystrom LM, Guzman ML, Rivella S. Iron and reactive oxygen species: friends or foes of cancer cells? Antioxidants Redox Signalling, 2014; 20: 1917-1924.
48. Jung M, Mertens C, Tomat E, Brüne B. Iron as a central player and promising target in cancer progression. Int J Mol Sci, 2019; 20:273.